A New RF Radiometer for Absolute Noninvasive Temperature Sensing in Biomedical Applications

AbdEl-Monem M. El-Sharkawy[1,2]
Paul P. Sotiriadis[1]
Department of Electrical Engineering[1]
Johns Hopkins University
Baltimore, Maryland USA

Paul A. Bottomley[1,2]
Ergin Atalar[1,2]
Department of Radiology[2]
Johns Hopkins University
Baltimore, Maryland USA

Abstract—Temperature sensing using microwave radiometry has proven value for non-invasively measuring the absolute temperature of tissues inside the human body. However, current clinical radiometers operate in GHz or infrared frequency ranges; this limits their depth of penetration since the human body is not "transparent" at these frequencies. To address this problem, we have designed and built an advanced, near-field radiometer operating at VHF frequencies (64MHz) with a ~100 KHz bandwidth. In the core of the radiometer lie an embedded impedance analyzer and an automatic antenna matching network; they compensate in-real time for any load variation that may occur due to near-field antenna coupling and movements of the human body. The radiometer has performed accurate temperature measurements to within ±0.1ºC, over a tested physiological range of 28-40ºC in saline phantoms whose electric properties match those of human tissue. The current method has the potential of being integrated on Magnetic Resonance Imaging (MRI) modalities.

I. INTRODUCTION

Over the past 30 years, radiometry has been used to measure the temperature of biological tissues in human and animal models. Being a passive detection modality, it does not require exposure to radiation and so it is both safe and entirely non-hazardous. Because fast-growing tumors can exhibit local temperature elevations over surrounding normal tissues, microwave radiometry has shown promise as a possible diagnostic tool for early breast cancer detection [1].

Of importance to the diagnostic utility of radiometry is the depth of tissue whose temperature measurements are being sought. The depth of penetration of EM radiation in human tissue decreases with frequency. Thus, radio frequencies (RF) below 200MHz are best suited for radiometry of tissues lying 1-20 cm deep in the body. Current clinical microwave radiometers operate at the GHz frequency range. Their architecture is typically based on Dicke's 1946 radiometer [2]. They are commonly built with a receiving antenna connected to a circulator and/or an isolator to reduce inaccuracy due to load variation (Figure 1).

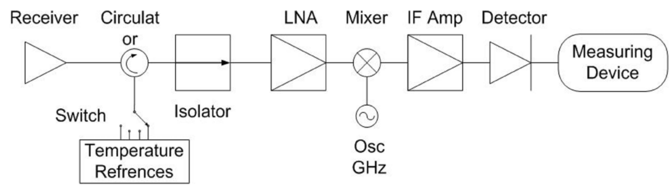

Figure 1. Typical microwave radiometer architecture: the signal (noise) received by the antenna passes through the circulator and the isolator that compensate for any mismatch. The signal is then amplified by a low noise amplifier and then down-converted to a lower frequency and filtered. The measuring device at the end estimates the RMS power of the signal (noise).

In this work we have built a radiometer that operates at 64MHz in order to achieve higher depth of penetration and be compatible with 1.5T MRI scanners [4]. Accurately measuring radiated noise power at low RF frequencies (and small bandwidths) is challenging because the received signal has relatively less available power and the antenna operates in the near-field making the reception very sensitive to movement and

This work was supported by the National Institute of Health (NIH) grants R01HL57483, and R01RR15396.

1-4244-0921-7/07 $25.00 © 2007 IEEE.

Authorized licensed use limited to: Univ of Calif San Diego. Downloaded on October 18, 2008 at 14:55 from IEEE Xplore. Restrictions apply.

environmental changes. Also, isolators and circulators are impractical due to their physical sizes at such frequencies.

In our system, the antenna (coil) used for receiving noise radiation is precisely matched with an accuracy of 0.05 Ω to 50Ω to compensate for load variations, using automatic vector impedance sensing. After impedance-matching the antenna is switched to an amplifier where the received noise power is amplified and measured. Based on the received signal the temperature of a body lying in the antenna's (near-field) region of sensitivity is estimated. As in standard microwave radiometers, our system requires calibration against known temperature loads. We demonstrate the measurement of absolute temperatures on a phantom of comparable EM properties to biological tissue over a physiological temperature range.

II. Theory

The main concept of RF radiometry is based on the well-known theory of black body radiation as described by Nyquist [3]. The equation governing this phenomenon for a typical receiver chain is

$$P = (1-\Gamma^2)G(\Gamma(T))KBT + N(\Gamma(T)) \quad (1)$$

Where P is the measures radiated noise power, G is the power gain of the antenna receiver, Γ is the reflection coefficient at the antenna-body interface (near-field coupling), k is the Boltzman constant, T is the temperature of the body in Kelvin, B is the system's bandwidth, and N is the noise power added by the receiver. In lumped form, this relation can be written as,

$$P = \alpha(\Gamma)T + \beta(\Gamma) \quad (2)$$

Where α and β are unknown lumped system parameters. When Γ is constant, the system parameters (α, β) are fixed and can be derived by calibration using known temperature loads.

III. Impedance Matching

In order to keep Γ constant, precise measurement of the sample's (body) loading to the antenna (coil) is central to the radiometer's operation. The impedance of the antenna (near-field) is modeled under the expected loading conditions using a lumped equivalent circuit.

A pi-network was used to match the antenna (coil) to 50Ω as illustrated in Figure 2: the exact model parameters are tabulated therein. The simulated performance of the (automatically tuned) matching network under various loading conditions of the antenna (coil) over the 100KHz bandwidth is shown in Figure 2(b).

Figure 2(d) shows the variation in magnitude of the antenna's (coil) impedance after the matching network, with respect to 50Ω, as a function of Cm2 and Cm3 for the antenna (coil) loading conditions shown in the first row of the table in Figure 2(c). The function has a unique minimum within the operating range thus enabling automatic matching. Figure 2(e) shows the π matching network along with the low-pass filters for the varactors' control lines entering the E/M shielded box containing the RF electronics. Additional filters used on the control lines are shown in Figure 2(f).

In order to accurately measure the impedance seen after the matching network it is (selectively) connected to a Maxwell bridge whose output is fed to a quadrature mixer (Figure 3). The output voltage vector (V_I, V_Q), after the mixing and filtering, is related to the real and imaginary impedance difference (ΔR, ΔX) from 50Ω by

$$\begin{bmatrix} V_I \\ V_Q \end{bmatrix} = \frac{\zeta V_i}{200} \begin{bmatrix} \cos\varphi & -\sin\varphi \\ \sin\varphi & \cos\varphi \end{bmatrix} \begin{bmatrix} \Delta R \\ \Delta X \end{bmatrix} \quad (3)$$

where φ is the phase of the voltage source V_i and where ζ is the gain of the amplification stage.

Authorized licensed use limited to: Univ of Calif San Diego. Downloaded on October 18, 2008 at 14:55 from IEEE Xplore. Restrictions apply.

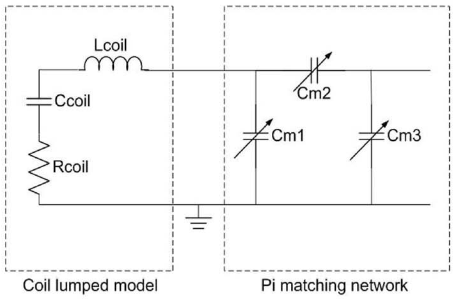

A

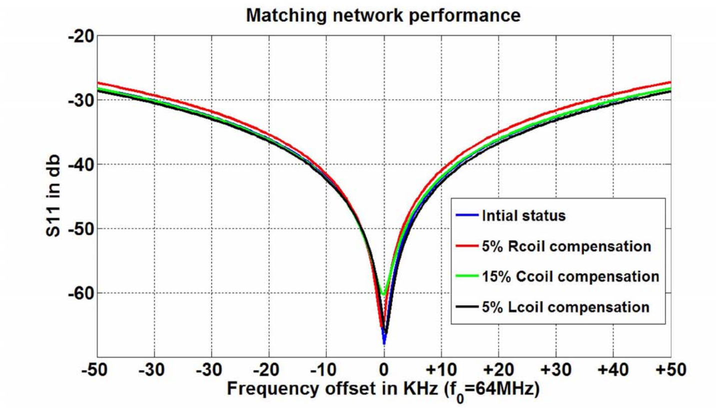

B

	Rcoil	Ccoil	Lcoil	Cm1	Cm2	Cm3
Initial Matched	2	30	248	91.5	127.5	83
5% ΔRcoil	1.8	30	248	91.5	120.5	88.7
15% ΔCcoil	2	35	248	45	62	109
5% ΔLcoil	2	35	236	59.5	73.8	95.5

C

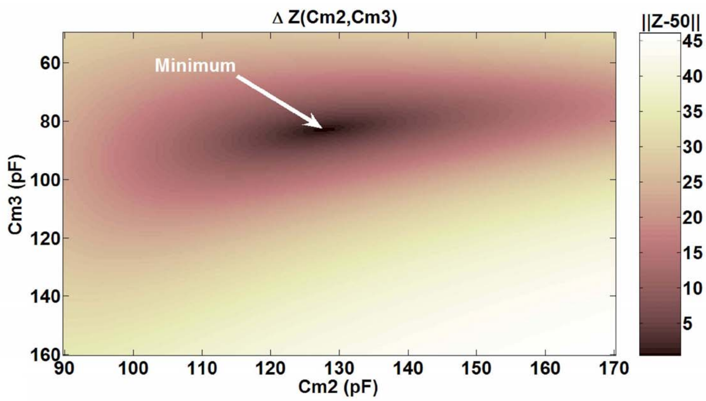

D

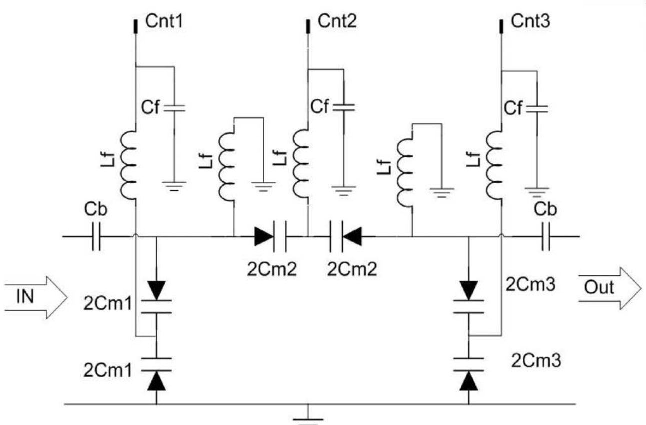

E

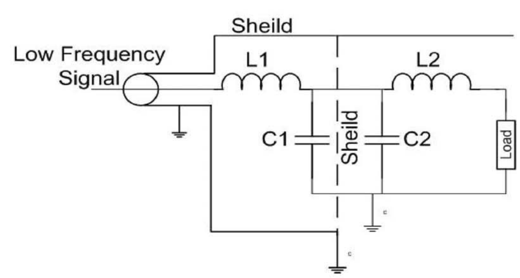

F

Figure 2. **A.** Equivalent model of the antenna (coil) and the impedance matching network. **B.** Curves showing matching performance over the 100 KHz band. **C.** Table showing the circuit parameters for curves shown in (B) where; Resistance is in Ω, Capacitance is in pF and Inductance in nH. **D.** Impedance error (after the matching network) as a function of Cm2 and Cm3 for the antenna (coil) loading conditions in the first row of the table in part (C). There exists a unique minimum within the operating range. **E.** Circuit diagram of the matching network. Very low serial resistance varactors are used for matching and their capacitance values are controlled via voltage lines Cnt1,2, and 3. **F.** Circuit diagram for an electric line going through the filter box.

Because of this transformation, before each impedance measurement the impedance sensing circuit is calibrated using three precision impedance reference loads. The antenna's (coil) impedance is then measured with an accuracy of 0.05Ω and electronically matched using the matching network. Using the accurate measurements of the antenna's (coil) impedance error, the voltages on the matching circuit varactors are tuned based on a heuristic modified gradient decent numerical algorithm with

Authorized licensed use limited to: Univ of Calif San Diego. Downloaded on October 18, 2008 at 14:55 from IEEE Xplore. Restrictions apply.

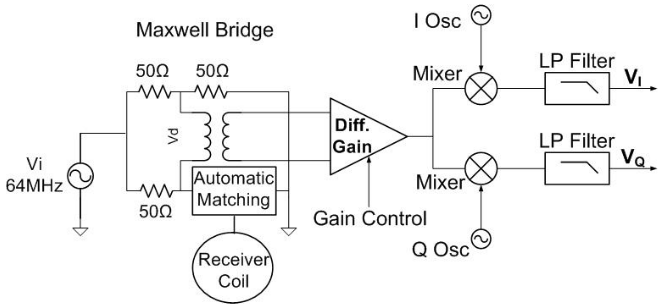

Figure 3. Block diagram for vector impedance sensing.

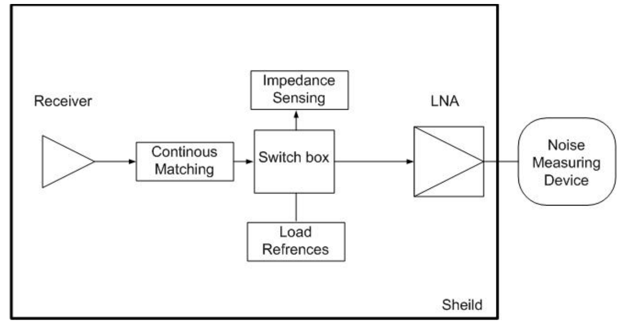

Figure 4. Bock diagram of the proposed RF radiometer.

an adaptive step. After the antenna (coil) is matched, it is connected (along with the matching network) to the amplification stage. A high level block diagram of the automated system is shown in Figure 4.

IV. RESULTS

After calibration, the radiometric system was tested with heated water phantoms prepared with different concentrations of saline. Phantom temperature was accurately controlled and monitored via an independent fiber-optic temperature sensing device connected to a heater. The radiometer was first calibrated against references of known temperature. After calibration, radiometric temperature measurements were performed and compared with the independent sensor measurements (Figure 5). The calculated RMS error over four studies shows an accuracy of $\pm 0.1^0$C in temperature estimation [4].

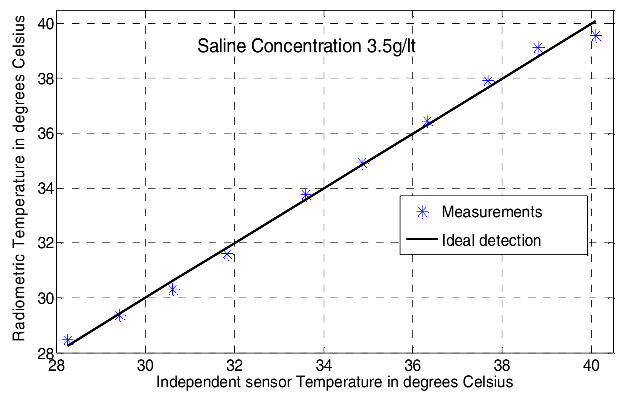

Figure 5. Temperature measured from noise power vs. temperature measured with accurate fiber optic thermometer.

V. CONCLUSION

We have demonstrated through phantom studies that the proposed RF radiometer, using continuous RF impedance sensing, matching and calibration, can be used to detect absolute temperature with an accuracy of $\pm 0.1^0$C over a physiological range.

The RF radiometer can potentially be used for monitoring the average absolute temperature of tissues lying much deeper in the body than can be detected with microwave radiometers.

ACKNOWLEDGMENT

The authors would like to thank Dr. Marion Lee Edwards, Director of RF Eng. group APL, for insightful technical comments.

REFERENCES

[1] K. Carr, "*Microwave Radiometry: Its Importance to The Detection of Cancer",* IEEE Trans. on Microwave Theory and Techniques, Vol. 37, No. 12, P.1862-1869, Dec.1989.

[2] R. Dickie, "*The Measurement of Thermal Radiation at Microwave Frequencies",* Rev. Sci. Instr., Vol. 17, P. 268-275, July 1946.

[3] H. Nyquist, "*Thermal Agitation of Electric Charge in Conductors",* Physical Review, Vol. 32, P. 110-112, July 1928.

[4] A. El-Sharkawy, P. Sotiriadis, P. Bottomley, E. Atalar, *"Absolute Temperature Monitoring using RF Radiometry in the MRI Scanner"*, IEEE Trans. on Circuits & Systems-I, Vol. 53, No. 11, Nov. 2006, pp. 2396–2404.

Authorized licensed use limited to: Univ of Calif San Diego. Downloaded on October 18, 2008 at 14:55 from IEEE Xplore. Restrictions apply.